Discontinuities in the Nuclear Mass Surface

ALEX E. S. GREEN* AND DAVID F. EDWARDS
Department of Physics, University of Cincinnati, Cincinnati, Ohio
(Received December 18, 1952)

Proton and neutron binding energies are analyzed in such a way as to permit an approximate assessment of the effects associated with pairing and shell structure. We draw several interesting conclusions with respect to the accuracy of various theoretical expressions which have been proposed for the pairing effect. Our analysis of the data and considerations of an atomic model lead us to a simple approximate representation of a shell stabilizing correction to nuclear energies. This shell structure term accounts rather well for the observed departures from the general trends of beta-stability, nuclear masses, and nuclear Q values. Our shell correction suggests that much larger systematic variations in nuclear masses may be identified with shell structure effects than might previously have been suspected.

1. THE DATA AND THEIR INTERPRETATION

IT has been pointed out in the preceding paper[1] that nuclear mass decrements can be represented fairly accurately by the smooth function:

$$\Delta_m{}^r(A)=(A-100)^2/100-64, \text{ (mMU)}. \quad (1)$$

To facilitate the analysis of the discontinuities in the experimental mass surface, we have converted the experimental data into a set of mass residuals and reaction energy or Q-value residuals. The mass residual, in mMU, for a particular nuclide is here defined as

$$R=\Delta-\Delta_m{}^r(A), \quad (2)$$

where Δ is the experimental mass decrement ($\Delta=M-A$). The Q-value residual is defined [GE Eq. (20)] as:

$$R(Q)=Q-Q_m{}^r(A). \quad (3)$$

By referring the mass decrements and Q values to $\Delta_m{}^r(A)$ and $Q_m{}^r(A)$ instead of the complete reference functions, we greatly simplify the task of computing residuals. At the same time we still have the advantages of reference functions which are good approximations to the actual functions.

For studying shell and pairing discontinuities in the nuclear mass surface, we shall assume that the mass residuals may be represented by

$$R(N,Z)=S_{ij}(N,Z)+P(N,Z)+J^o[D-D_m{}^o(A)]^2. \quad (4)$$

The subscript i is used to denote a region of the mass surface lying between the planes defined by the magic neutron number N_u and N_l and the subscript j is used to denote a region lying between planes defined by the magic proton numbers Z_u and Z_l. (See Table II or Fig. 6.) $S_{ij}(N,Z)$ is assumed to embody the shell structure effect and $P(N,Z)$ is now used to represent the pairing effect. We shall assume that

$$\begin{aligned} &P(O,O)=H, \quad P(E,E)=-H, \\ &P(E,O)=p, \quad P(O,E)=n, \end{aligned} \quad (5)$$

where E and O denote the evenness or oddness of N or Z, respectively. We thus are adhering to the convention of referring masses to a surface which lies halfway between the even-even and odd-odd nuclear surfaces. We now allow, however, for the possible departures of the two odd mass surfaces from this intermediate surface. The parabolic term contains the optimum smooth functions for the line of stability and the parabolic width.

When both the target and product nuclides belong to the same zone, the Q-value residual is

$$R(Q)=S_{ij}(N,Z)-S_{ij}(N',Z')+P(N,Z)-P'(N',Z')+J^o\theta^2-J^{o\prime}\theta'^2, \quad (6)$$

where

$$\theta=D-D_m{}^o(A) \quad \text{and} \quad \theta'=D'-D_m{}^o(A').$$

Since the change in N, Z, and A are usually small compared to N, Z, and A we may express this equation approximately as

$$R(Q)\approx(n'-n)\partial S_{ij}/\partial N+(z'-z)\partial S_{ij}/\partial Z+P-P'+J^o(\theta^2-\theta'^2), \quad (7)$$

where n, n', z, and z' are the neutron and proton numbers of the incident and ejected particles. Thus apart from the spin and parabolic effect residual Q values are related to the partial derivatives of the shell function. The problem of opportioning the residual Q values to the four terms on the right side of Eq. (7) is complicated by the fact that these terms are frequently of the same order of magnitude. Fortunately by the judicious choice of data for study the problem becomes tractable.

2. NEUTRON AND PROTON BINDING ENERGIES

Neutron and proton binding energies furnish a good source of data for studying shell effects since in these cases either the first or second term in Eq. (7) vanishes. Neutron and proton binding energies may be obtained from

$$B_n(N,Z)=\Delta(N-1,Z)+\Delta_n-\Delta(N,Z)=-Q[X(\gamma,n)X'] \quad (8)$$

* Now at the Department of Physics, Florida State University, Tallahassee, Florida.

[1] A. E. S. Green and N. A. Engler, preceding paper [Phys. Rev. 91, 40 (1953)]; hereafter referred to as GE.

and

$$B_p(N,Z)=\Delta(N,Z-1)+\Delta_H-\Delta(N,Z)$$
$$=-Q[X(\gamma,p)X']. \quad (9)$$

To obtain the residual neutron binding energy we subtract $Q_m{}^r$ from both sides of Eq. (8). We find

$$R_n(N,Z)=B_n(N,Z)-B_n{}^r(A), \quad (10)$$

where $B_n{}^r(A)$ is the negative of the $Q_m{}^r(A)$ for the γ, n reaction. Using GE Eq. (17), it is simple to show that

$$R_n(N,Z)=R(N-1,Z)-R(N,Z). \quad (11)$$

Similiarly, for the residual proton binding energy,

$$R_p(N,Z)=B_p(N,Z)-B_p{}^r(A) \quad (12)$$
$$=R(N,Z-1)-R(N,Z). \quad (13)$$

$B_n{}^r(A)$ and $B_p{}^r(A)$ are reference functions found in Table III GE.

An extensive collection of neutron binding energies from (γ, n) thresholds, from the Q values of (n, γ) reactions, and (d, p) reactions, and from mass data is available.[2] However, few proton binding energies have been measured directly. The residual proton binding energies may be computed from (p, γ) reactions, (d, n) reactions and mass residual data using Eqs. (12) and (13) or else by the use of

$$R_p(N,Z)=R_n(N,Z)$$
$$+[R(N,Z-1)-R(N-1,Z)] \quad (14)$$

which follows from Eqs. (11) and (13). Since the difference between the mass residuals indicated in brackets is the same as the difference between masses this term may frequently be obtained from beta decay energies.

In view of Eqs. (8) and (9) we have, as special cases of Eq. (7),

$$R_n(N,Z)=-\partial S_{ij}/\partial N+P'-P+J^o(\theta'^2-\theta^2), \quad (15)$$

and

$$R_p(N,Z)=-\partial S_{ij}/\partial Z+P'-P+J^o(\theta'^2-\theta^2). \quad (16)$$

The parabolic term presents considerable difficulties. Not only is it a tedious term to compute but it is particularly sensitive to small fluctuations in the location of the valley. Since the shell effect is probably the main cause of fluctuations in the line of stability, we find ourselves in the situation of having to know the shell correction in order to evaluate the shell correction. Fortunately a successive approximation approach helps to resolve the difficulty. The approach which we adopted is based upon an attempt to minimize the parabolic term by selecting pairs of nuclides which have at least one β-stable member. Since the change in θ associated with the removal of a neutron or proton is of the order of $+1$ or -1, respectively, the difference of the squares may be expected to be a positive or negative number of the order of unity. Consequently the parabolic correction term is of the order of $25/A$, which is relatively small for medium and heavy nuclides although appreciable for light nuclides. Accordingly we must expect, particularly for small A, scattering of the points from any smooth curve which represents the shell and spin corrections.

[2] *Nuclear Data*, National Bureau of Standards, Circular 499 (U. S. Government Printing Office, Washington, D. C., 1950) and Supplements appearing in Nuclear Science Abstracts.

TABLE I. The pairing correction to binding energies.

	Neutron binding			Proton binding		
N, Z	$\tau\neq\pi+\nu$	$\tau=\pi+\nu$	$\pi=\nu=H$	$\tau\neq\pi+\nu$	$\tau=\pi+\nu$	$\pi=\nu=H$
E, E	ν	ν	H	π	π	H
O, O	$-\tau+\pi$	$-\nu$	$-H$	$-\tau+\nu$	$-\pi$	$-H$
E, O	$\tau-\pi$	ν	$+H$	$-\pi$	$-\pi$	$-H$
O, E	$-\nu$	$-\nu$	$-H$	$\tau-\nu$	$+\pi$	H

It has been pointed out that the pairing correction represents the additional energy due to unpaired nucleons. If the reference surface is taken as the *EE* surface, we may denote the additional energies of an *EO*, *OE*, or *OO* nuclide as π, ν, and τ, respectively. These are the same π and ν as used by Coryell and Suess.[3] To allow for the possible interaction of the odd proton and odd neutron, we have not restricted our τ to $\pi+\nu$. In Table I we show an analysis of the pairing correction for the binding energies of protons and neutrons as they depend upon the nuclear type given in column one. In columns 2 and 5 we indicate the pairing energy differences involved in these cases under the general assumption that the pairing energies take on the values 0, π, ν and τ. In columns 3 and 6 we indicate what these differences would be if $\tau=\pi+\nu$. In columns 4 and 7 we indicate what these differences would be if $\pi=\nu=\tau/2=H$.

Ignoring momentarily the parabolic and pairing corrections, the neutron and proton binding energy residuals [Eqs. (15) and (16)] are just the negatives of the partial derivatives of the shell structure term. On plots of R_n *vs* N and R_p *vs* Z the points corresponding to the nuclides should collect about the curves $-\partial S_{ij}/\partial N$ and $-\partial S_{ij}/\partial Z$, respectively. Taking into account the pairing term of Eq. (15) and (16) we would expect, if $\tau=\pi+\nu$, that the experimental points will be above or below $-\partial S_{ij}/\partial N$ and $-\partial S_{ij}/\partial Z$ by the distances given in columns 3 and 6 of Table I. Accordingly, the points on the R_n *vs* N plot should group in such a way that the curve $-\partial S_{ij}/\partial N$ would be half-way between the average distributions of the *EE*, *EO* group and the *OO*, *OE* group. Similiarly for the R_p *vs* Z plot, the average distribution curves for the *EE*, *OE* group and the *OO*, *EO* group should be equally spaced about the $-\partial S_{ij}/\partial Z$ curve. We must expect random scattering about these distribution curves because of the parabolic factor. The distance between these average distribution curves on the R_n and R_p plots is expected to be 2ν and 2π, respectively. On the other hand, if τ differs from $\pi+\nu$ we would in both cases find four curves spaced

[3] C. D. Coryell and H. E. Suess, Phys. Rev. **86**, 609 (1952).

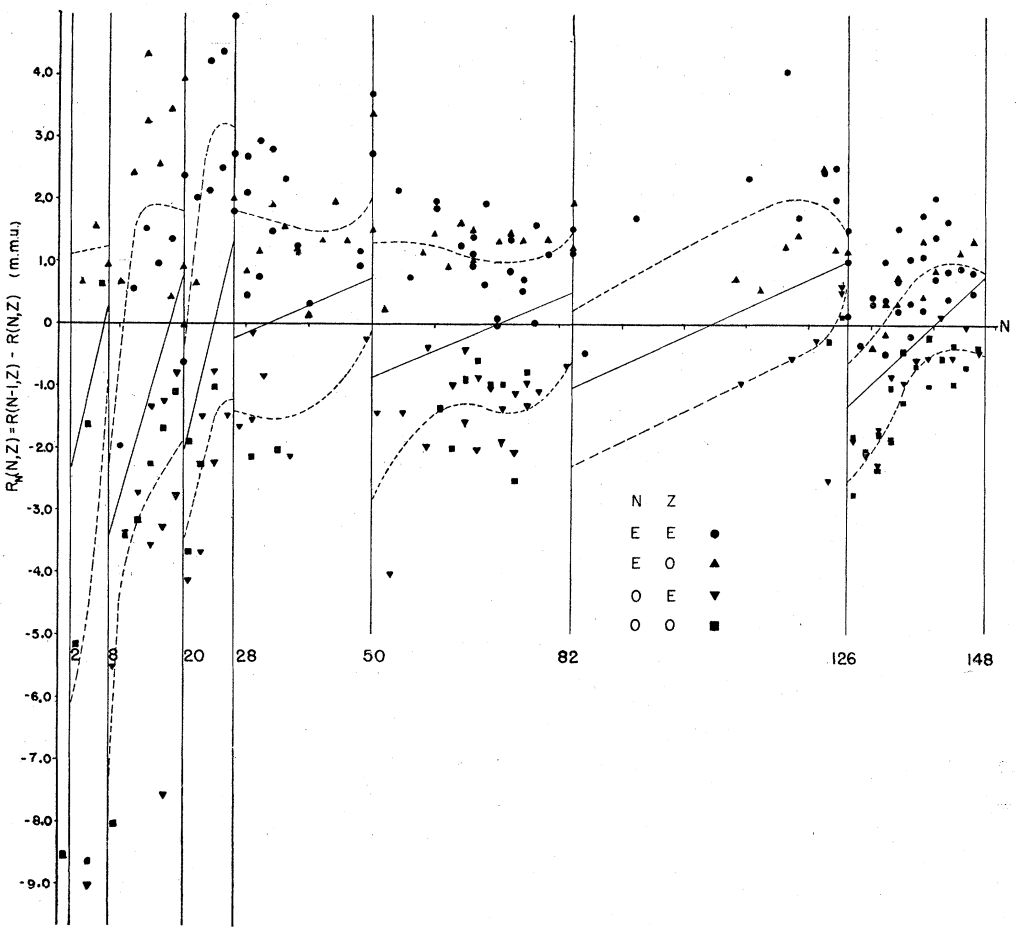

FIG. 1. The residual neutron binding energy *vs* neutron number. The points are designated as to the type, i.e., the evenness or oddness of the number of neutrons or protons. The grouping of the *EE* and *EO* types and the grouping of the *OO* and *OE* types can be seen. The dashed curves indicate the average distributions of these groups. The solid line represents our visual estimate of the best straight line representation of $-(\partial S_{ij}/\partial N)$. The $-(\partial S_{ij}/\partial N)$ which we use in Sec. 4 consists of a series of straight line segments running from -1 at the lower magic number to 1 at the upper magic number.

with respect to $-\partial S_{ij}/\partial N$ and $-\partial S_{ij}/\partial Z$ in accord with the columns 2 and 5 of Table I.

The neutron and proton binding energy residuals computed from recent experimental data[2] are shown in Figs. 1 and 2, respectively. To accommodate the computed residuals different vertical scales were used in Figs. 1 and 2.

3. THE PAIRING EFFECT

If we examine Figs. 1 and 2 we observe that to a large extent the grouping of types expected on the basis of the assumption that $\tau=\pi+\nu$, is fulfilled. In several instances significant departures seem to occur. The most noteworthy is in the region of A values between 230 and 240 where $\tau-(\pi+\nu)\approx 1$ mMU.

In Fig. 3 we have plotted pairing energies, experimental and empirical, as functions of the mass number. The corresponding N and Z numbers computed from the reference line of beta-stability $\{N_m{}^r(A)=\frac{1}{2}[A+D_m{}^r(A)]$, $Z_m{}^r(A)=\frac{1}{2}[A-D_m{}^r(A)]\}$ are also shown. The squares and the circles represent estimated values of π and ν, respectively, for five-unit intervals of N and Z. These values have been obtained from an analysis of the separation of the types in Fig. 1 and Fig. 2.

In Eq. (5) we take as a reference the surface which lies halfway between the *EE* and *OO* surfaces. For the case $\pi\neq\nu$ we may let $H=\frac{1}{2}(\pi+\nu)$. Various functions of A have been proposed for this pairing correction. In Fig. 3 we show three of these functions, $H_1(A)=140/A$,[4] $H_2(A)=36/A^{\frac{3}{4}}$,[5] and $H_3=10/A^{\frac{1}{2}}$.[6] Of these three the last appears to best follow the variation with A. The function $12/A^{\frac{1}{2}}$ is probably still better although it is somewhat smaller in the middle range than the experimental data indicate.

[4] S. Glasstone, *Source Book on Atomic Energy* (D. Van Nostrand Company, Inc., New York, 1950). The pairing function suggested by J. W. Blatt and V. F. Weisskopf in *Theoretical Nuclear Physics* (John Wiley and Sons, Inc., New York, 1952) is quite close to this one.

[5] E. Fermi (unpublished).

[6] A. E. S. Green, Phys. Rev. **86**, 654 (1952).

Mayer,[7] on the assumption of a delta-function attractive potential for the spin orbit coupling model, obtains formulas for the pairing energy which may be expressed as

$$\pi = -C(j_\pi + \tfrac{1}{2})/A \qquad (17)$$

and

$$\nu = -C(j_\nu + \tfrac{1}{2})/A, \qquad (18)$$

where j_π or j_ν is the total angular momentum of each proton or neutron in a given subshell and $C \sim 25$ Mev. These values of π and ν are also plotted in Fig. 3. π is represented by the dashed lines and ν by the dash-dot lines. We have based our j values on the spin orbit model as represented by the specific level scheme of Klinkenberg.[8] We have used only the average A for a particular subshell since according to Eqs. (17) and (18) the variation in π or ν within a subshell is small. For the moment we cannot say that Eqs. (17) and (18) are consistent with our experimental estimates of π and ν. The fact that Eqs. (17) and (18) are not inconsistent with the experimental values suggests that we must ultimately abandon efforts to represent the pairing effect by the simple functions of mass number which are in common use.

The values of $\pi - \nu$ as found from the circles shown in Fig. 3 are in agreement, on the whole, with the values given by Coryell.[9]

4. A REFERENCE SHELL CORRECTION

From the scattering of the points in Figs. 1 and 2 it is obvious that a variety of $-\partial S_{ij}/\partial N$ and $-\partial S_{ij}/\partial Z$ curves may be chosen. To proceed further in our attempt to find a suitable representation of shell effects, we have elected to represent these curves by the series of straight line segments. This representation is not only suggested by the proton and neutron binding energy data but it is also suggested by the irregularities in the corresponding ionization energy data in the atomic case.[10] Accordingly, we shall assume that between any two major magic numbers we have

$$-\partial S_{ij}/\partial N = 2\alpha_i(N - N_i) \qquad (19)$$

and

$$-\partial S_{ij}/\partial Z = 2\alpha_i(Z - Z_j), \qquad (20)$$

where α_i and α_j are proportional to the slopes of these straight line segments and N_i and Z_j are constants which must be adjusted for each region. In effect we have chosen to represent the shell correction by the series of functions

$$S_{ij}(N, Z) = -\alpha_i(N - N_i)^2 - \alpha_j(Z - Z_j)^2 + k_{ij}. \qquad (21)$$

Our shell function thus has the shape of an inverted cup with the peak value at N_i and Z_j, points which usually lie intermediate between the boundaries of the zone.[11] In Table II we list the values of α_i, N_i, α_j, and Z_j obtained from a visual adjustment of the straight line segments in Figs. 1 and 2.

Let us now consider the manner in which the addition of a shell term given by Eq. (21) alters a mass decrement surface which has the basic form

$$\Delta(A, D) = \Delta_m(A) + J[D - D_m(A)]^2. \qquad (22)$$

Since the semi-empirical equation may be placed in this form our discussion is applicable to these equations as

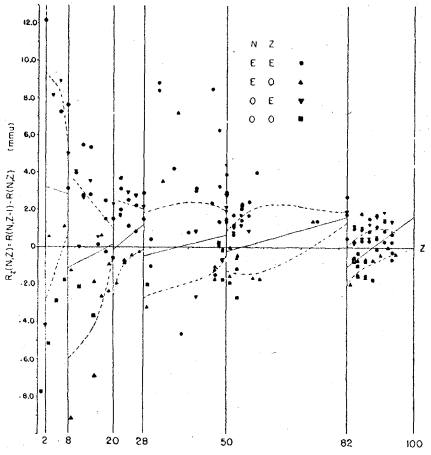

FIG. 2. The residual proton binding energy *vs* proton number. The points are designated as to the type, i.e., the evenness or oddness of the number of neutrons and protons. The grouping of the *EE* and *OE* types and the grouping of the *OO* and *EO* types can be seen. The dashed curves indicate the average distributions of these groups. The solid line represents our visual estimate of the best straight line representation of $-(\partial S_{ij}/\partial Z)$. The $-(\partial S_{ij}/\partial Z)$ which we use in Sec. 4 consists of a series of straight line segments running from -1 at the lower magic number to 1 at the upper magic number.

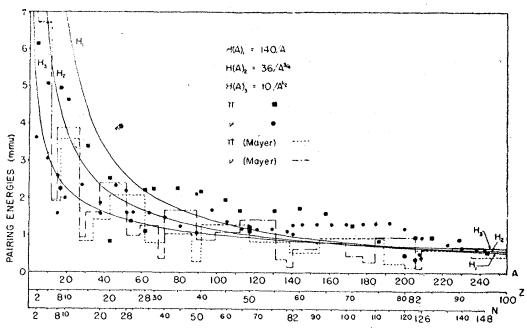

FIG. 3. The pairing energies of the last nucleon are plotted as a function of the mass number. The N and Z scales correspond to values which lie along our reference line of beta-stability. The experimental pairing energies (ν and π) as estimated from Figs. 1 and 2 are indicated by the solid circle and square, respectively. The pairing functions of mass number given by Glasstone, Fermi, and Green are represented by the solid curves.

[7] M. G. Mayer, Phys. Rev. **78**, 22 (1950).
[8] P. F. A. Klinkenberg, Revs. Modern Phys. **24**, 63 (1952).
[9] C. D. Coryell *Annual Reviews of Nuclear Science* (Annual Reviews, Inc., Stanford, 1953), Vol. II.
[10] See Fig. 6.3, H. E. White, *Introduction to Atomic Spectra* (McGraw-Hill Book Company, Inc., New York, 1934).
[11] A. H. Wapstra, Physica **18**, 83 (1952) has proposed a shell stabilizing term which is quite different from that proposed here. Our shell stabilizing term has the advantage of introducing sharp breaks in the line of betas-tability which is considered to be essential by Coryell (reference 9).

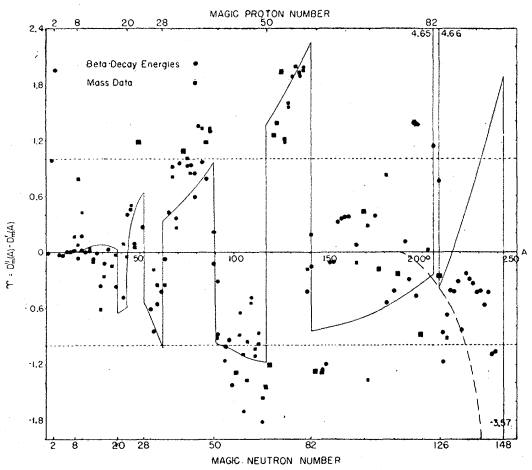

FIG. 4. Location of beta-stability point *vs* mass numbers. The circles and squares indicate the points computed on the basis of experimental data. The solid line represents the line of stability computed on the basis of our reference shell correction and our smooth reference line of beta-stability. The dashed line indicates the change in the smooth baseline apparently needed in the very heavy region.

well as to our reference equation. Letting

$$N=\tfrac{1}{2}(A+D_m+D-D_m)=N_m(A)+\tfrac{1}{2}(D-D_m), \quad (23)$$

and

$$Z=\tfrac{1}{2}(A-D_m-D+D_m)=Z_m(A)-\tfrac{1}{2}(D-D_m), \quad (24)$$

and inserting these into the sum of Eq. (21) and Eq. (22), we find it is possible to express the result in each zone in the form of Eq. (22) if we let

$$\Delta_m{}^{ij}(A)=\Delta_m(A)-\alpha_i[N_m(A)-N_i]^2 -\alpha_j[Z_m(A)-Z_j]^2+k_{ij}-\frac{1}{4J^{ij}(A)} \times\{\alpha_i[N_m(A)-N_i]-\alpha_j[Z_m(A)-Z_j]\}^2, \quad (25)$$

$$D_m{}^{ij}(A)=D_m(A)+[\alpha_i(N_m-N_i) -\alpha_j(Z_m-Z_j)]/2J^{ij}(A) \quad (26)$$

and

$$J^{ij}(A)=J(A)-(\alpha_i+\alpha_j)/4. \quad (27)$$

Rather than go further with the extensive set of empirical constants listed in Table II, we may without introducing considerable error replace these constants by the slightly different set:

$$\bar{\alpha}_i=(N_u-N_l)^{-1}\ \text{mMU}, \quad \bar{\alpha}_j=(Z_u-Z_l)^{-1}\ \text{mMU},$$
$$\bar{N}_i=(N_u+N_l)/2, \quad \bar{Z}_j=(Z_u+Z_l)/2, \quad (28)$$

where the subscripts u and l refer to the upper and lower magic numbers of the particular zone. In using these simple expressions for the parameters in our shell correction, we have exploited the latitude now available to us in view of the scattered data. Essentially we are representing the shell structure function by the expression:

$$S_{ij}(N,Z)=-\frac{1}{N_u-N_l}\left(N-\frac{N_u+N_l}{2}\right)^2 -\frac{1}{Z_u-Z_l}\left(Z-\frac{Z_u+Z_l}{2}\right)^2+k_{ij}. \quad (29)$$

This expression, which of course must be treated only as a first approximation, has the distinct advantage of requiring only one empirical constant for each zone other than the magic numbers themselves. Using our smooth reference functions, we shall now investigate the extent to which this reference shell function may account for effects attributed to shell structure. *Since our reference functions are "averages" of the semi-empirical functions much of this discussion pertains to these latter functions also.*

5. THE SHELL CORRECTION AND THE LINE OF BETA-STABILITY

In the preceding paper[1] (see Fig. 3), marked irregularities were noted in the function Υ which characterizes the deviations of the true line of stability from the reference function $D_m{}^r(A)$. To arrive at a more precise curve for Υ, we shall present the results of an analysis based upon beta decay energies and mass data rather than stability limits. Let $D_m{}^{ij}(A)$ denote the true minimum of an isobaric section at mass number A. If we ignore the π, ν difference the mass difference between adjacent odd mass isobaric nuclides is

$$M^*-M_s=J^{ij}(A)\{[D^*-D_m{}^{ij}(A)]^2 -[D_s-D_m{}^{ij}(A)]^2\}, \quad (30)$$

where the asterisk denotes a radionuclide and the subscript s the stable nuclide. Since $D^*=D_s\pm 2$, this becomes

$$M^*-M=4J^{ij}(A)\{1\pm[D-D_m{}^{ij}(A)]\} =\gamma^{ij}[1\pm(\theta-\Upsilon)]100/A, \quad (31)$$

TABLE II. Shell correction parameters.

i	N_l	N_u	α_i	N	$\bar{\alpha}_i$	$\bar{N}$
1	0	2			0.300	1
2	2	8	0.22	7	0.1667	5
3	8	20	0.18	18	0.0834	14
4	20	28	0.22	25	0.125	24
5	28	50	0.023	33	0.0455	39
6	50	82	0.022	70	0.0312	66
7	82	126	0.023	104	0.02275	104
8	126	148	0.048	140	0.0455	137
j	Z_l	Z_u	α_j	Z	$\bar{\alpha}_j$	$\bar{Z}$
1	0	2			0.500	1
2	2	8			0.1667	5
3	8	20	0.05	19	0.0834	14
4	20	28	0.088	21	0.125	24
5	28	50	0.023	40	0.0455	39
6	50	82	0.030	53	0.0312	66
7	82	100	0.075	88	0.0555	91

where here

$$\theta = D - D_m{}^r(A) \tag{32}$$

and

$$\Upsilon = D_m{}^{ij}(A) - D_m{}^r(A). \tag{33}$$

If two mass differences are known we may set up two equations and solve Eq. (31) for r^{ij} and Υ for a given isobaric section. Unfortunately apart from the region of heavy nuclides there are only a few instances in which two mass differences are known for odd isobars. In order to make some use of the extensive data corresponding to odd mass isobars for which only one mass difference is known, we have for these cases as a reasonable first approximation let $r^{ij}=1$ (see GE, Fig. 5) and solved this one equation for Υ.

In Fig. 4 we show the location of the minimum mass points of odd mass nuclides which have been computed using a recent collection of beta decay energies (circles) and our set of mass values (squares). Also shown in Fig. 4 is the difference $\Upsilon = D_m{}^{ij} - D_m{}^r(A)$ computed using Eq. (26) and Eq. (28). It is clear from the plot that in the main the experimental points do fluctuate in accord with the predictions based upon our reference shell function. The agreement may be improved even further if in the very heavy region $D_m{}^r(A)$ were taken as the dotted curve indicated in Fig. 4.

6. SHELL CORRECTION AND THE NUCLEAR MASSES

The constants, k_{ij}, in Eq. (21) are still to be determined. Substituting S_{ij} from Eq. (21) into Eq. (4) we have

$$R(N,Z) = -\bar{\alpha}_i(N-\bar{N}_i)^2 - \bar{\alpha}_j(Z-\bar{Z}_j)^2 + k_{ij} + J^o\theta^{o2} + P. \tag{34}$$

For odd-mass beta-stable nuclides the pairing term and parabolic term will be small so that the constants, k_{ij}, can be evaluated approximately by substituting the data appropriate for these nuclides. Using the values of $\bar{\alpha}_i$, $\bar{\alpha}_j$, $\bar{N}_i$, and $\bar{Z}_j$ from Table II as well as a table of $R(N,Z)$ values computed from recent mass data we have calculated the various k_{ij} values. In this computation we have noted that for a particular zone, i.e., a specific i and j, the computed value of k_{ij} varied somewhat. The k_{ij} at shell edges derivated the greatest from the average; accordingly, values of $R(N,Z)$ for either magic N or magic Z or both were not included in the final computation of k_{ij}. The values of k_{ij} so calculated checked rather closely wlth a set obtained by a graphical method. Our estimated values of k_{ij}, are listed in Table III. To test this set of k_{ij} values and the remainder of the shell correction we plotted in Fig. 5:

TABLE III. Estimated k_{ij} values in mMU.

i,j	2,2	3,2	3,3	4,3	4,4	5,4
k_{ij}	−2.5	2.5	3.0	7.0	3.5	2.5
i,j	5,5	6,5	6,6	7,6	8,7	
k_{ij}	5.5	6.5	8.0	3.5	1.5	

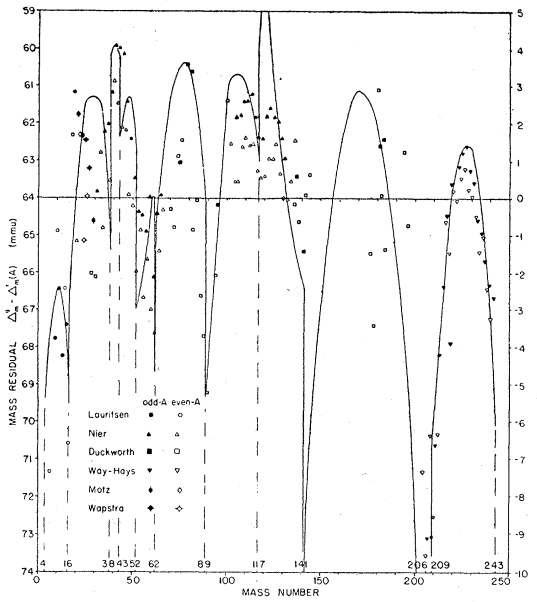

FIG. 5. The mass residuals for beta-stable nuclides *vs* mass number. The solid symbols represent odd-A nuclides and open symbols the even-A nuclides. The symbols used designated the source of experimental data (see references 6–12 in GE). The discontinuous curve represents the mass residuals for the beta-stable points of a surface which incorporates our smooth reference functions and our reference shell stabilizing term. The left vertical scale denotes residuals computed with respect to $\Delta_m{}^r(A) = (A-100)^2/100$, whereas the right vertical scale denotes residuals computed with respect to $\Delta_m{}^r(A) = (A-100)^2/100 - 64$.

$$\begin{aligned}\Delta_m{}^{ij}(A) - \Delta_m(A) &= -\frac{1}{N_u - N_l}\left[N_m(A) - \frac{N_u+N_l}{2}\right]^2 - \frac{1}{Z_u - Z_l} \\ &\times\left[Z_u(A) - \frac{Z_u+Z_l}{2}\right]^2 + k_{ij} - \frac{1}{4J^{ij}(A)} \\ &\times\left\{\frac{1}{N_u - N_l}\left[N_m(A) - \frac{N_u+N_l}{2}\right]^2 \right. \\ &\left. - \frac{1}{Z_u - Z_l}\left[Z_m(A) - \frac{Z_u+Z_l}{2}\right]\right\}^2. \end{aligned} \tag{35}$$

The function represented by Eq. (35) is discontinuous at the magic A numbers. These discontinuities are probably not entirely significant, since our shell term is expected to be inaccurate at these shell edges. If in following the atomic model we had joined a nuclide corresponding to a closed shell with a straight line segment to the nuclide with a closed shell plus one neutron or proton in our curves for $-\partial S_{ij}/\partial N$ and $-\partial S_{ij}/\partial Z$, we would have avoided these discontinuities. The residual masses of beta-stable odd-mass nuclides should fall fairly close to this curve except at shell edges.

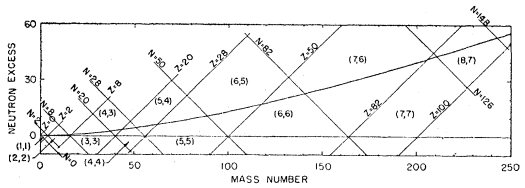

FIG. 6. The line of beta-stability in relationship to zones defined by magic numbers. The numbers in parentheses are the indices of the zone (i, j).

On the other hand, the beta-stable even-mass nuclides, which we included because there are not enough odd-mass nuclides to test our curve, should fall somewhat below ($\sim$1 mMU) the curve representing Eq. (35). An examination of Fig. 5 shows that on the whole these features are borne out by the evidence. The magnitude of the scattering of the points is probably greater than can be attributed to experimental error, to the pairing effect or to the parabolic effect. Thus unquestionably there is room for improvement in the shell stabilizing term.

7. THE SHELL CORRECTION AND Q VALUES

Accepting Eq. (21) as the shell correction, we readily find that for reactions with the target and product nuclides in the same zone

$$Q_s=2\alpha_i(n-n')(N-N_i)+\alpha_i(n-n')^2 +2\alpha_j(z-z')(Z-Z_i)+\alpha_i(z-z')^2. \quad (36)$$

Using the simplified set of constants [Eq. (28)] this becomes

$$Q_s=2(n-n')(N-\bar{N}_i)/(N_u-N_l) +2(n-n')^2/(N_u-N_l) +2(z-z')(Z-\bar{Z}_j)/(Z_u-Z_l) +2(z-z')^2/(Z_u-Z_l), \quad (37)$$

an equation which is quite simple to handle. To test the accuracy of our complete reference surface we have computed Q values of numerous (γ, n) and alpha-decay reactions. Upon comparing these predicted values with the (γ, n) threshold values given by Sher,[12] and the α-decay energies given by Perlman and Seaborg,[13] we found that 67 percent of our predictions were within 1 mMU of the experimental value. This represents a substantial improvement in accuracy with respect to predictions based upon our smooth reference function alone, or the semi-empirical mass functions.

8. CONCLUSION

Our study of the discontinuities of the experimental mass surface has led us to certain conclusions regarding pairing discontinuities and shell discontinuities.

We have examined the frequently accepted assumption that pairing effects may be represented by $+H(A)$, $-H(A)$, and zero for OO, EE, and (OE and EO) nuclides, respectively, where $H(A)$ is $36/A^{\frac{3}{4}}$ or $140/A$. We find this assumption to be untenable for the following reasons: (1) These functions exaggerate the average magnitude of the pairing effect for light nuclides. The function $12/A^{\frac{1}{2}}$ probably furnishes a closer representation of the average magnitude of the pairing effect. (2) The additional energy of unpaired neutrons or unpaired protons with respect to even N even Z nuclides differ in many regions, i.e., frequently $\pi \neq \nu$. (3) In some regions the energies associated with unpaired particles are non-additive. This suggests that an appreciable pairing interaction is present in OO type nuclides.[14] (4) The expressions for the pairing effect involving shell quantum numbers which were derived by Mayer using the shell model are not inconsistent with the available evidence. In view of the many successes of the shell model, it would seem that the final pairing correction will of necessity embody shell quantum numbers and hence will not be representable as a simple function of A, N, or Z.

In our study of the shell discontinuities we have found evidence that the shell effect upon neutron and proton binding energies may be approximately represented by a series of straight line segments between major magic numbers. This representation is also suggested by the general nature of the discontinuities in atomic ionization energies. Because the available data and our method of analysis did not permit a precise assignment of the parameters which characterize these straight line segments, we chose to study the consequences of a uniquely defined set of straight line segments which we found to be a not unreasonable representation of the available evidence. Pursuing this representation we deduced a shell stabilizing correction to nuclear energies which we found gives a rather good account of the departures from the general trends of beta-stability, nuclear masses, and nuclear Q values.

Perhaps the most startling conclusion to which we are led from this approximate representation is the large variation of masses which may be identified with a shell stabilizing term. The fact that in most regions where accurate mass values are available the line of beta-stability cuts the corners of shell zones, has tended to obscure this feature of the experimental mass surface. Only in the heavy region do we meet a situation where we can gauge the true range of the shell correction from the doubly magic corner of the zone to the peak. In Fig. 6 we indicate how our reference line of beta-stability (which is a fairly good one) crosses with respect to zones defined by magic N and magic Z numbers. We may conclude therefore that shell effects do greatly distort the masses of beta-stable nuclides from what they would be in the absence of shell effects. Accordingly theoretical expressions based upon the statistical theories of the nucleus must be adjusted to mass values

[12] Sher, Halpern, and Mann, Phys. Rev. **84**, 387 (1951).
[13] Perlman, Ghiorso, and Seaborg, Phys. Rev. **77**, 26 (1950).
[14] K. Way and M. Wood, Phys. Rev. **86**, 608 (1952) have noted an n-p interaction above Pb^{208} which is probably related to this.

which are substantially different from the actual masses of nuclides.

Unquestionably a better representation can be found for the shell stabilizing term than our present one. The local adjustment of the parameters incorporated in Eq. (21) probably would lead to a substantial improvement. It is also probable that the true shell correction may embody semimagic numbers and curved segments. At this time the experimental data is too sparse and too inaccurate in many regions of the mass surface to offer great encouragement to an effort to refine the shell correction on the basis of purely empirical considerations. Of necessity such a study will be a tedious one, since it will have to be made in conjunction with a more precise representation of the smooth trends of the nuclear mass surface and a more precise representation of the pairing effect than the simple expressions which we have used thus far. It appears therefore that we have reached a point at which we might best look to current nuclear theories to find a better representation of the shell stabilizing term.

We would like to express our appreciation to R. B. Minogue, N. J. Marucci, R. Oppenheim, J. S. Nader, N. Engler, R. Oswald, and Mrs. W. Steiger for their assistance in this study, and to Dr. C. D. Coryell for sending us a manuscript prior to publication.

PHYSICAL REVIEW VOLUME 91, NUMBER 1 JULY 1, 1953

The Parameters for the Slow Neutron Resonance in Rhodium*

V. L. SAILOR
Brookhaven National Laboratory, Upton, New York
(Received March 30, 1953)

Measurements of the 1.26-ev resonance in rhodium have been made with a crystal spectrometer and the following values were obtained for the parameters: $E_0=1.260\pm0.004$ ev, $\sigma_0=(5000\pm200)\times10^{-24}$ cm², $\Gamma=0.156\pm0.005$ ev, $g\Gamma_n=(3.8\pm0.2)\times10^{-4}$ ev, and $\sigma_{fa}=(5.5\pm1.0)\times10^{-24}$ cm². The shape of the resonance agrees to very high accuracy with the one-level Breit-Wigner formula. The procedure is discussed for analyzing experimental data in cases where small corrections are required for instrument resolution and Doppler broadening.

I. INTRODUCTION

THE slow neutron resonance in rhodium at 1.26 ev offers a particularly favorable opportunity for studying the details of an absorption resonance. Several factors contribute to simplify greatly the analysis of this case: Rhodium is monoisotopic; the 1.26-ev resonance is well isolated from other resonances and presumably is not complicated by interference effects; the contribution to the cross section form resonant scattering is very small and may be neglected in the analysis; and the resonant energy lies within the range of very high resolution of modern neutron spectrometers.

Several previous measurements of the rhodium cross section have been made;[1–3] however, in these cases the instrument resolution was inadequate for a detailed analysis. The relatively high resolution which can be obtained with newer spectrometers has justified a remeasurement of the rhodium cross section. The purpose of these new measurements is to obtain accurate values of the Breit-Wigner parameters and to study the details of the shape of the resonance. The measurements reported below were made with the BNL crystal spectrometer, which has been described elsewhere.[4]

II. PROBLEMS IN ANALYZING DATA

The experimentally observed shape of a resonance differs from the "true" shape because of the distortion introduced by finite instrument resolution and by the Doppler broadening resulting from the thermal motion of the atoms in the specimen. The corrections required to account for these effects are appreciable even for cases of very high resolution and small Doppler broadening. The problem of fitting experimental data to a theoretical dispersion curve is greatly complicated by the need for the above corrections. As experimental technique advances and the data becomes more refined, the problem of finding an adequate and practical method of analysis becomes more pressing.

There are several possible approaches to the analysis problem. The "area" method of Havens and Rainwater,[5] which corrects for resolution, has recently been made more quantitative by Melkonian[6] and is now being extended to include the Doppler correction.[7,8] Another less elegant approach which could best be described as the "trial and error" method has been frequently used.[3,5,9] This consists of choosing trial values of the Breit-Wigner parameters and then computing the effect

* Research supported by the U. S. Atomic Energy Commission.
[1] Borst, Ulrich, Osborne, and Hasbrouck, Phys. Rev. **70**, 557 (1946).
[2] W. J. Sturm, Phys. Rev. **71**, 757 (1947).
[3] R. R. Meijer, Phys. Rev. **75**, 773 (1949).
[4] L. B. Borst and V. L. Sailor, Rev. Sci. Instr. **24**, 141 (1953).
[5] W. W. Havens, Jr., and J. Rainwater, Phys. Rev. **70**, 154 (1946).
[6] E. Melkonian, Phys. Rev. **90**, 362 (1953).
[7] G. v. Dardel and R. Persson, Nature **170**, 1117 (1952).
[8] E. Melkonian, Bull. Am. Phys. Soc. **28**, No. 3, 26 (1953).
[9] B. D. McDaniel, Phys. Rev. **70**, 832 (1946).